bioXAS and metallogenomics

XANES quantitative structural determination of the sandwich bis(naphthalocyaninato) cerium complex

Z. Y. Wu,[a,b]* Y. Tao,[a] M. Benfatto,[b] D. C. Xian[a] and J. Z. Jiang[c]

[a]Beijing Synchrotron Radiation Facility, Institute of High Energy Physics, Chinese Academy of Sciences, PO Box 918, 100039 Beijing, People's Republic of China, [b]Istituto Nazionale di Fisica Nucleare, Laboratori Nazionali di Frascati, PO Box 13, 00044 Frascati, Italy, and [c]Department of Chemistry, Shandong University, Jinan 250100, People's Republic of China.
E-mail: wuzy@ihep.ac.cn

The molecular structure of the sandwich double-decker bis(naphthalocyaninato) cerium complex was determined for the first time in a quantitative way using a new method of analysis of the Ce L_3-edge X-ray absorption near-edge structure (XANES) in the framework of the full multiple scattering theory. An average Ce—N bond length of 2.47 Å was determined. In this complex structure the pyrrole rings play the key role in the determination of the XANES spectral features, and the differences in bond lengths between the Ce atom and the eight pyrrole N atoms are 0.14 Å, addressing a significant distortion of these rings around cerium. These results may be used to study double-decker imidazole rings, present as the structure model in the photosynthesis center and in sandwich-structured lanthanide chlorophyll molecules.

Keywords: XANES; cerium sandwich complex with tetrapyrrole ligands; MS calculation.

1. Introduction

Porphyrins and phthalocyanines are structure analogues of macrocyclic tetrapyrrole ligands. They have fascinated scientists owing to their significant role in life, materials and energy sciences (Kadish *et al.*, 2000). In particular, they are essential to biological processes owing to their roles in chlorophyll proteins and heme proteins. For example, metal-substituted chlorophylls have been extensively studied because of their contribution to the elucidation of the photosynthesis mechanism (Jiang *et al.*, 2001, and references therein). The investigation of rare-earth phthalocyaninato and porphyrinato, especially the sandwich-type compounds, has been an attractive research direction for both chemists and materials scientists for a long time because of their application in many fields such as liquid crystals, molecular semiconductors, molecular magnetic, molecular electronics and non-linear optical materials (Hartwich *et al.*, 1998). Double-decker sandwich metal porphyrin complexes are special owing to their strong π–π interaction between two tetrapyrrole rings with a metal ion inserted, compared with their mono-tetrapyrrole counterparts. The sandwich bis(porphyrinato) cerium complex has been used as the structure model of a special pair of bacteriochlorophyll molecules in the bacterial photosynthesis reaction center (Buchler & Heinz, 1996). In particular, EXAFS (extended X-ray absorption fine structure) results have also confirmed that there exists a double-decker sandwiched structure in La-substituted chlorophyll extracted from the fern plant, *Dicranopteris dichotoma*, which is the

most rare-earth-element-concentrated plant, growing on the erosion layer of ion-adsorption rare-earth-element deposits in the south of China (Tao *et al.*, 2001).

Among the 14 stable lanthanide elements, cerium has the unique electronic configuration of $[Xe]4f^1 5d^1 6s^2$, which makes the chemistry of this metal very different from the others in the lanthanide series. Therefore, the homoleptic bis(naphthalocyaninato) cerium complex, $Ce[Nc(tBu)_4]_2$, was selected as the objective here.

X-ray absorption spectroscopy has been used in the studies of porphyrin and phthalocyaninato complexes (Goulon *et al.*, 2000), especially in hemeprotein studied by EXAFS (Andersson & Dawson, 1991). For sandwich complexes of tetrapyrrole ligands, however, only a few reports have been published, and these have mainly used the EXAFS method (Caminiti *et al.*, 1999; Agondanou *et al.*, 2001; Tao *et al.*, 2001). Furthermore, to the best of our knowledge, no quantitative study has ever been conducted, especially quantitative calculations of the X-ray absorption near-edge spectrum (XANES), for this kind of compound.

2. Methods

2.1. Calculations

We present the quantitative analysis of the Ce L_3-edge XANES spectrum performed by a new analysis procedure of *MXAN* that is able to fit the XANES part of the XAFS spectrum and has been used to investigate unknown systems

Table 1
Individual bond lengths (Å) between Ce and eight pyrrole N atoms.

Case 1 corresponds to the initial structure, case 2 to the fit considering Ce as an impurity and moving independently, and case 3 to the fit moving the eight Np atoms independently. R_{sq} is the value of the square residue.

Ce—Np	N1	N2	N3	N4	N5	N6	N7	N8	R_{sq}
Case 1	2.49 ± 0.02	2.49 ± 0.02	2.50 ± 0.02	2.50 ± 0.02	2.50 ± 0.02	2.51 ± 0.02	2.51 ± 0.02	2.51 ± 0.02	90.36
Case 2	2.42 ± 0.02	2.54 ± 0.02	2.45 ± 0.02	2.59 ± 0.02	2.42 ± 0.02	2.58 ± 0.02	2.47 ± 0.02	2.57 ± 0.02	39.49
Case 3	2.47 ± 0.02	2.44 ± 0.02	2.52 ± 0.02	2.41 ± 0.02	2.53 ± 0.02	2.47 ± 0.02	2.38 ± 0.02	2.50 ± 0.02	10.50

over the last three years (Della Longa *et al.*, 2001, 2003; Benfatto *et al.*, 2002; Benfatto & Wu, 2003; Cardelli *et al.*, 2003; Sepulcre *et al.*, 2004). This method, which is described in detail by Benfatto *et al.* (2004), is based on the comparison between the experimental spectrum and several theoretical calculations generated by changing the relevant geometrical parameters of the site. The X-ray absorption cross sections are calculated using the full multiple scattering scheme in the framework of the muffin-tin (MT) approximation; in other words, the scattering path operator is calculated exactly (Natoli & Benfatto, 1986). The construction of the charge density and potential follows the same patterns as that in Wu *et al.* (1996, 2004). We use the Mattheiss prescription (Mattheiss, 1964) to construct the cluster density. The Coulomb part of the potential is obtained by superposition of neutral atomic charge densities taken from the Clementi–Roetti tables (Clementi & Roetti, 1974). For the exchange-correlation part of the potential, we have used the optical Hedin–Lundqvist potential (Hedin & Lundqvist, 1969, 1971; Lee & Benni, 1977; Chou *et al.*, 1987, and references therein). In order to simulate the charge relaxation around the core hole in the photoabsorber of atomic number Z (Ce = 58), we select the $Z + 1$ approximation (final state rule) (Lee & Benni, 1977) which consists of taking the orbitals of the $Z + 1$ atom and constructing the charge density by using the excited electronic configuration of the photoabsorber with the core electron promoted to a valence orbital. The calculated spectra are further convoluted with a broadening Lorentzian-shaped function, with a full width given by $\Gamma = \Gamma_c + \Gamma(E)$. The constant part includes the core-hole lifetime (3.4 eV; Fuggle & Inglesfield, 1992) and the experimental resolution (1.2 eV), while the energy-dependent term represents all the inelastic processes. The $\Gamma(E)$ function is zero below an onset energy E_s, and it starts to increase from a value A_s following the universal functional form of the mean free path in a solid (Muller *et al.*, 1984). MT radii are chosen according to the Norman criterion (Norman, 1974; Joly, 2001).

2.2. Experiments

XANES at the Ce L_3 edge was measured in transmission mode by using synchrotron radiation with a Si(111) double-crystal monochromator at beamline 4W1B of the Beijing Synchrotron Radiation Facility (BSRF). The storage ring was working at the typical energy of 2.2 GeV with an average electron current of about 100 mA. To suppress the unwanted harmonics, a detuning of 40% was performed between the two silicon crystals. The spectra were recorded at room temperature with two ionization chambers, filled with nitrogen in the front and a 25% argon-doped nitrogen mixture in the back. The microcrystalline powder sample was pressed into a thin pellet of appropriate thickness for a jump edge around 1.0. The energy position was calibrated using a third ionization chamber.

The sample was synthesized as follows. *n*-Octanol was distilled from sodium. The compounds 6-*tert*-butylnaphthalo-nitrile and Ce(acac)$_3$·H$_2$O were prepared following published procedures (Kovshev *et al.*, 1971; Sites *et al.*, 1948). The cerium complex Ce[Nc(tBu)$_4$]$_2$ was prepared by using the previously reported method (Nyokong *et al.*, 2000).

3. Results and discussions

The starting model for the geometrical arrangement of atoms around the Ce ion was taken from the La(Por)(Pc) structure model constructed by the three-dimensional builder of the Cerious 2 module after consulting the molecular structure studies of the sandwich lanthanoid porphyrin complex (Buchler *et al.*, 1986; Buchler & Cian, 1988). The Ce ion is surrounded by eight N atoms of the two naphthalocyanine rings, and its coordination polyhedron is almost a square antiprism. The four pyrrole N atoms (Np) of each of the macrocycles are almost coplanar. The eight Ce—Np bond lengths do not significantly differ from each other and have a mean value of 2.50 Å (see Table 1).

The shell parameters are obtained within a 5 Å range from the central Ce ion. This range is sufficient for data analysis because most of the main contributions come from the pyrrole rings within a 5 Å scope. The model was minimized in energy for a chemically reasonable structure. In Fig. 1 the experimental spectrum (circles) and the best fit result (solid line) are shown. This fit was initially carried out with a fixed geometrical structure. The MS calculation reproduces all the main features of the experimental spectrum, indicating that the atomic cluster, containing 49 atoms (photoabsorber and two C$_{20}$N$_4$ macrocycles), is large enough to characterize qualitatively the spectral features. However, the mismatch between the experimental data and the MS calculation reflects that the environment around the Ce ion used should be different from the initial structure.

For this reason we have begun the fitting procedure by considering the Ce atom as an impurity and moving in *x*, *y*, *z* independently, *i.e.* the two macrocycles are forced to move jointly during the procedure (all eight Np are linked). The comparison between the experimental data (open circles) and the calculated result (solid line) is presented in Fig. 2 and
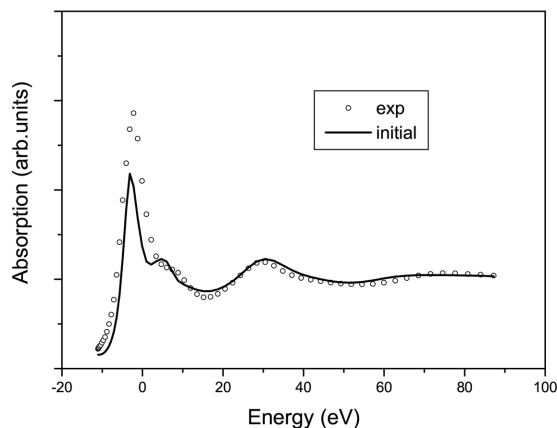
Figure 1
Theory-*versus*-experiment best-fit results obtained starting from the original geometrical structure and varying the potential parameters.
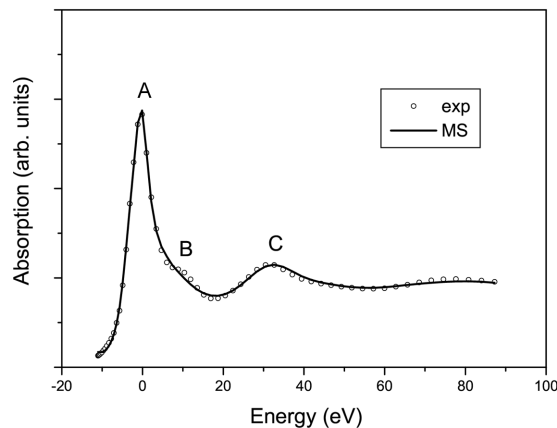

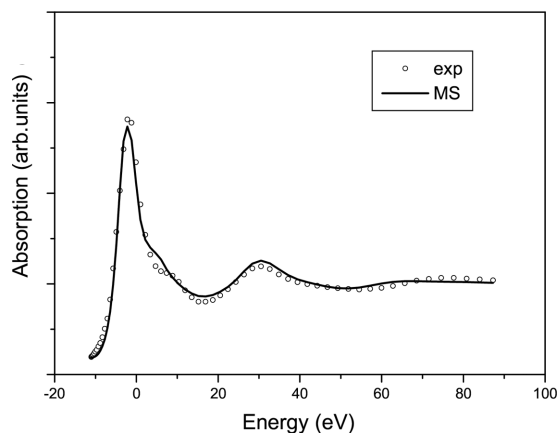**Figure 2**
Theory-*versus*-experiment best-fit results obtained by considering the Ce atom as an impurity and moving in *x*, *y*, *z* independently.

Figure 3
Theory-*versus*-experiment best-fit results obtained by moving the eight Np atoms independently.

Figure 4
Final double-decker sandwich structured cluster of the Ce phthalocyaninato and porphyrinato complex obtained by *MXAN* best-fit. The central atom Ce is surrounded by eight Np atoms (blue atoms).

clearly shows the high sensitivity of the XANES spectroscopy to the geometrical arrangement of the atoms. The best-fit condition corresponds to the two naphthalocyanine rings with a mean cerium–nitrogen distance of 2.51 Å. Individual values of the Ce—N bond distances are summarized in Table 1.

As expected, the agreement between the experimental data and the fitting calculations is good in the energy range from the spectral onset to 90 eV, while relevant discrepancies are still present at lower energy, between −10 eV and 35 eV, owing to the constraint condition on all eight Np atoms.

In Fig. 3 we report a comparison between the experimental data (open circles) and the calculated result (solid line) obtained by moving all the first-shell atoms without any linkage, *i.e.* with the eight Np atoms moving independently. The best agreement between the calculation and the experimental results is reached over the whole energy range with an average Ce—N bond length of 2.47 Å, confirming the possibility of recovering the correct geometrical environment around the absorbing site. The minimization procedure converged on a mean displacement of about 0.01 Å. However, the distortion of Ce—Np from the average value is significant (about 0.06 Å) and the differences in the Ce—Np bond length
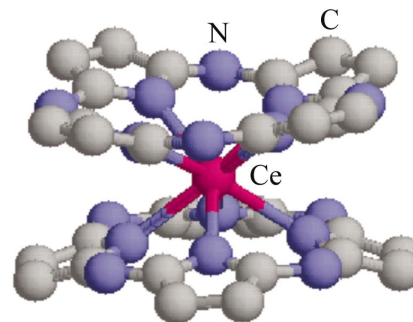
are about 0.14 Å, addressing a significant distortion of these rings around cerium. All characteristic spectral features, labeled A, B and C, are very well reproduced, indicating that there is only the Ce^{3+} contribution in the investigated system. The peak B arises predominately from structure distortion. The final double-decker sandwich structure obtained by *MXAN* calculations is shown in Fig. 4. All best-fit parameters and the values of the square residue (R_{sq}) are reported in Table 1.

4. Conclusion

For the first time, a quantitative analysis of the Ce L_3-edge XANES spectrum of the sandwich-structured naphthalocyanine complex has been carried out at atomic resolution, by a full multiple scattering approach. Our XANES analysis has allowed a complete determination of the lanthanide-ligand geometry. It is the first report of a detailed lanthanide sandwich structure of naphthalocyanines at atomic resolution from XANES to the best of our knowledge.

Our results indicate that not only can XANES provide the electronic properties information that it usually does but it can also provide the quantitative geometry information at the atomic level, which is vital in the elucidation of the double-

decker porphyrin rings, present as the structure model in the bacterial photosynthesis reaction center and in sandwich-structured lanthanide chlorophyll molecules. Also our results will be useful in handling units which are affected by multiple scattering which are extensive in metalloproteins, such as imidazole, where, like the pyrrole ring in porphyrin, there exists extensive multiple scattering owing to the forward-scattering enhancement.

As this manuscript can be considered as a preliminary work, we have not taken into account the effects of the tilting angle between the two macrocycles. We will refine the structure and extract the correlation information between the fitted Ce−N bond lengths and the tilting angles in the near future using the new *MXAN* code.

References

Agondanou, J.-H., Spyroulias, G. A., Purans, J., Tsikalas, G., Souleau, C., Coutsolelos, A. G. & Benazeth, S. (2001). *Inorg. Chem.* **40**, 6088–6096.

Andersson, L. A. & Dawson, J. H. (1991). *Metal Complexes with Tetrapyrrole Ligands II*, edited by J. W. Buchler, pp. 1–407. Berlin: Springer-Verlag.

Benfatto, M., D'Angelo, P., Della Longa, S. & Pavel, N. V. (2002). *Phys. Rev. B*, **65**, 174205/1–174205/5.

Benfatto, M., Della Longa, S., Qin, Y. W., Li, Q. L., Pan, G., Wu, Z. Y. & Morante, S. (2004). *Biophys. Chem.* **110**, 191–201.

Benfatto, M. & Wu, Z. Y. (2003). *Nucl. Sci. Techn.* **14**, 9–19.

Buchler, J. W. & Cian, A. D. (1988). *Inorg. Chem.* **27**, 342–347.

Buchler, J. W., Cian, A. D., Fischer, J., Kihn-Botulinski, M., Paulus, H. & Weiss, R. (1986). *J. Am. Chem. Soc.* **108**, 3652–3659.

Buchler, J. W. & Heinz, G. (1996). *Chem. Ber.* **129**, 1073–1078.

Caminiti, R., Donzello, M. P., Ercolani, C. & Sadun, C. (1999). *Inorg. Chem.* **38**, 3027–3029.

Cardelli, A., Cibin, G., Benfatto, M., Della Longa, S., Brigatti, M. F. & Marcelli, A. (2003). *Phys. Chem. Miner.* **30**, 54–58.

Chou, H., Rehr, J. J., Stern, E. A. & Davidson, E. R. (1987). *Phys. Rev. B*, **35**, 2604–2614.

Clementi, E. & Roetti, C. (1974). *Atom. Data Nucl. Data Tables*, **14**, 177–236.

Della Longa, S. A., Arcovito, A., Benfatto, M., Congiu-Castellano, A., Girasole, M., Hazemann, J. L. & Lo Bosco, A. (2003). *Biophys. J.* **85**, 549–558.

Della Longa, S. A., Arcovito, A., Girasole, M., Hazemann, J. L. & Benfatto, M. (2001). *Phys. Rev. Lett.* **87**, 155501–155504.

Fuggle, J. C. & Inglesfield, J. E. (1992). *Unoccupied Electronic States, Topics in Applied Physics*, Appendix B, p. 347. Berlin: Springer.

Goulon, J., Goulon-Ginet, C. & Gotter, V. (2000). *X-ray Absorption Spectroscopy Applied to Porphyrin Chemistry. The Porphyrin Handbook*, Vol. 7, edited by K. M. Kadish, K. M. Smith and R. Guilard, pp. 80–166. San Diego: Academic Press.

Hartwich, G., Fiedor, L., Simmonin, I., Cmiel, E., Schafer, W., Noy, D., Scherz, A. & Scheer, H. (1998). *J. Am. Chem. Soc.* **120**, 3675–3683.

Hedin, L. & Lundqvist, S. (1969). *Solid State Phys.* **23**, 1–181.

Hedin, L. & Lundqvist, S. (1971) *J. Phys. (Paris)*, C4, 2064–2083.

Jiang, J. K., Kasuga, K. & Arnold, D. P. (2001). *Supramolecular Photo-sensitive and Electro-Active Materials*, edited by H. S. Nalwa, ch. 2, pp. 113–210. New York: Academic Press.

Joly, Y. (2001). *Phys. Rev. B*, **63**, 125120/1–125120/10.

Kadish, K. M., Smith, K. M. & Guilard, R. (2000). Editors. *The Porphyrins Handbook. Applications: Past, Present and Future*, Vol. 6. San Diego: Academic Press.

Kovshev, E. I., Puchnova, V. A. & Luk'yanets, E. A. (1971). *Zh. Org. Khim.* **7**, 369–371.

Lee, P. A. & Benni, G. (1977). *Phys. Rev. B*, **15**, 2862–2883.

Mattheiss, L. (1964). *Phys. Rev. A*, **133**, 1399–1403.

Muller, J. E., Jepsen, O. & Wilkins, J. W. (1984). *Solid State Commun.* **42**, 4331–4343.

Natoli C. R. & Benfatto, M. (1986) *J. Phys. (Paris)*, **47**, C8–11.

Norman, J. G. (1974). *Mol. Phys.* **81**, 1191–1198.

Nyokong, T., Furuya, F., Kobayashi, N., Du, D., Liu, W. & Jiang, J. (2000). *Inorg. Chem.* **39**, 128–135.

Sepulcre, F., Proietti, M. G., Benfatto, M., Della Longa, S., Garcia, J., & Padros, E. (2004). *Biophys. J.* **87**, 513–520.

Sites, J. G., McCarty, C. N. & Quill, L. L. (1948). *J. Am. Chem. Soc.* **70**, 3142–3143.

Tao, Y., Zhao, G., Yang, J., Ikeda, S., Jiang, J., Hu, T., Chen, W., Wei, Z. & Hong, F. (2001). *J. Synchrotron Rad.* **8**, 996–997.

Wu, Z. Y., Ouvrard, G., Lemaux, S., Moreau, P., Gressier, P., Lemoigno, F. & Rouxel, J. (1996). *Phys. Rev. Lett.* **77**, 2101–2105.

Wu, Z. Y., Xian, D. C., Natoli, C. R., Marcelli, A., Mottana, A. & Paris, E. (2001). *Appl. Phys. Lett.* **79**, 1918–1920.